Nota Técnica

OPTIMIZATION AND PRACTICAL IMPLEMENTATION OF ULTRAFAST 2D NMR EXPERIMENTS

Luiz H. K. Queiroz Júnior*
Departamento de Química, Universidade Federal de São Carlos, Rod. Washington Luís, km 235, 13565-905 São Carlos – SP /
Instituto de Química, Universidade Federal de Goiás, CP 131, 74001-970 Goiânia – GO, Brasil
Antonio G. Ferreira
Departamento de Química, Universidade Federal de São Carlos, Rod. Washington Luís, km 235, 13565-905 São Carlos – SP, Brasil
Patrick Giraudeau
Université de Nantes, CNRS, Chimie et Interdisciplinarité: Synthèse, Analyse, Modélisation UMR 6230, B.P. 92208, 2 rue de la
Houssinière, F-44322 Nantes Cedex 03, France

Ultrafast 2D NMR is a powerful methodology that allows recording of a 2D NMR spectrum in a fraction of second. However, due to the numerous non-conventional parameters involved in this methodology its implementation is no trivial task. Here, an optimized experimental protocol is carefully described to ensure efficient implementation of ultrafast NMR. The ultrafast spectra resulting from this implementation are presented based on the example of two widely used 2D NMR experiments, COSY and HSQC, obtained in 0.2 s and 41 s, respectively.

Keywords: ultrafast 2D NMR; COSY; HSQC.

INTRODUCTION

Analysis of the historical panorama of Nuclear Magnetic Resonance (NMR) reveals great evolution of this phenomenon[1-3] since the first records. Part of this impressive evolution is due the emergence of two-dimensional (2D)[4,5] and imaging[6,7] experiments. In spite of this progress, conventional multidimensional NMR experiments still require a high number of scans to sample the indirect t_1 domain, leading to long experiment durations (from several minutes to several hours). This limitation creates not only timetable constraints, but also renders conventional nD NMR experiments unsuitable for the study of kinetic or dynamic phenomena occurring on a short timescale or for hyphenated techniques such as LC-NMR. Several methodologies have been proposed to overcome this limitation in order to obtain spectra in shorter time frames,[8-12] most notably the technique proposed by Frydman *et al.*,[13] also known as "ultrafast NMR" (UF-NMR). This technique allows performing of multidimensional experiments in a single scan, provided that sensitivity is sufficient.

The approach of UF-NMR differs to that used in its conventional counterpart, in terms of spin evolution and data acquisition. In a conventional 2D NMR experiment, spins are uniformly excited and t_1 evolution is systematically incremented in a series of distinct experiments. Acquisition is carried out by the storage of different FIDs (Free Induction Decays) from the corresponding incremented experiments.[5] In the UF-NMR approach, the usual t_1 encoding is replaced by spatial encoding, and after a conventional mixing period, the spatially encoded information is decoded by a detection block based on echo planar imaging (EPI).[7] The principles of UF-NMR have been extensively described in recent reviews[14-16] and are summarized below.

The spatial encoding scheme initially proposed by Frydman[13,17] relies on a succession of frequency-selective pulses applied during alternating bipolar gradient pairs. However, it suffers from several drawbacks as it requires fast gradient switching, carefully synchronized with RF irradiation. Moreover, it leads to the appearance of undesirable "ghost peaks"[18] in the indirect domain. Consequently,

this discrete excitation scheme was replaced by several continuous encoding patterns[19-22] relying on the combination of continuous frequency swept pulses applied during a bipolar gradient. The most efficient approach in terms of resolution and sensitivity is probably that proposed by Pelupessy (Figure 1S, supplementary material),[20] where spatial encoding is carried out in a constant-time manner through the application of two chirp pulses concomitantly with a bipolar gradient pair (G_e). The first pulse/gradient combination results in quadratic dephasing (z^2) which requires the application of z^2 gradients for refocusing of the magnetizations arising from different z positions. An alternative consists of applying, following the first pulse, an identical pulse together with an opposite gradient. This leads to linear dephasing that depends linearly on position along the z axis and resonance frequency (W_1). It should also be noted that in this excitation scheme, spatial encoding is performed in a constant-time manner. Briefly, we can imagine the sample being divided into infinitesimal slices with dephasing varying linearly according to position.

The mixing step remains exactly the same as that used in conventional experiments,[13,20] preserving the linear dephasing obtained by the previous encoding block. For acquisition, a scheme based on echo planar imaging (EPI)[7] is used. Firstly, after the receiver is open, the acquisition gradient G_a (with duration of a few hundred microseconds) is applied to refocus the dephasing acquired in the course of spatial encoding, leading to the formation of a series of echoes whose positions are proportional to the resonance frequencies that have been encoded (Figure 2S-a, supplementary material), where the signals observed during this period are similar to an 1D spectrum. As a consequence, the first dimension of the 2D spectrum, also called the "ultrafast dimension", is obtained without any Fourier Transform.

In order to obtain the second dimension, alternated $\pm G_a$ gradients (Figure 2S-b, supplementary material) are applied, typically during one hundred milliseconds, to monitor the spin evolution in the course of the t_2 acquisition time under the effect of classical parameters: resonance frequency, transverse relaxation, J-couplings, etc. These alternated gradients induce a series of refocusings and defocusings, which results in a set of symmetrical 1D spectra (mirror-image echoes). As the conventional interactions are characteristic of this

*e-mail: professorkeng@gmail.com

dimension, it is generally called a "conventional dimension". After data rearrangement and FT along t_2, a 2D spectrum is obtained containing the same information as its conventional counterpart.

Many studies have been performed to improve the performances of this promising technique, in terms of sensitivity,[23] resolution,[24,25] lineshape,[26] and accessible spectral width.[26,27] Following these improvements, UF-NMR has been applied successfully in a broad range of domains, including the study of mechanistic,[28] kinetic[29] or dynamic[30] processes, the coupling with *ex-situ* Dynamic Nuclear Polarisation[31] or the application to quantitative analysis.[32] Nevertheless, due to the numerous non-conventional parameters involved in this methodology and to the specific processing required, its implementation is no trivial task. In this context, the aim of the present paper was to describe the practical protocol used in the implementation of this technique to record UF-NMR spectra. The main difficulties regarding the implementation of this powerful tool are described, based on the example of two widely used 2D NMR experiments: COSY and HSQC.

EXPERIMENTAL

Sample preparation

For the initial calibration of encoding gradients and pulses, a 600 µL solution of H_2O/D_2O (90:10) was prepared. For the conventional and ultrafast COSY experiments, Levamisol (purchased from Sigma-Aldrich) solution was obtained by dissolving 10 mg of this compound in 600 µL of MeOD. The concentrated solution used for the conventional and ultrafast HSQC experiments was prepared by mixing 200 µL of 1-bromohexane in 400 µL of $CDCl_3$. All these samples were filtered and transferred to 5 mm tubes. Deuterated solvents were purchased from Cambridge Isotope Laboratories, Inc.

General NMR parameters

All the NMR experiments were performed at 298 K on a Bruker Avance III 400 spectrometer, operating at a frequency of 400.15 MHz ^1H, with a 5mm SmartProbe® with gradients along the *z*-axis (50 G/cm for 100% gradient amplitude). For both conventional and ultrafast experiments, the pulse width for $\pi/2$ pulse was 8.13 ms for ^1H and 15.0 µs for ^{13}C.

Ultrafast 2D NMR parameters

The main acquisition parameters for calibration of encoding gradients were set as follows: time domain size - 2984 data points (real + imaginary); spectral width - 300 ppm; acquisition time - 10 ms; number of scans - 1; central frequency - H_2O peak; duration of refocusing gradient (G_1) - 10 ms; delay between π pulse and G_1 - 1 ms; acquisition gradient delay (d_{ag}) - 5 ms; G_1 strength - 4 G/cm; hard pulse duration - calibrated as for the conventional experiments. The d_{ag} delay was adjusted to place the echo in the center of the acquisition window. For processing, an apodization function was applied with LB (Lorentzian-Broadening) of -20 Hz and GB (Gaussian-Broadening) at the position of the echo, *i.e.* 0.5. A Fourier transform (FT) was then done, followed by phase correction. This last step is crucial because of the phase dispersion induced by the gradients, therefore it was first performed by first order phase correction (typically 70000°), and finally by a small zero order correction to obtain a symmetric image.

For the calibration of encoding pulses, an adiabatic pulse with a smoothed chirp shape was created (10% smoothing), with a frequency range of 60 kHz, 10% higher than the frequency dispersion induced by the 6.77 G/cm excitation gradient (G_e), and with 15 ms duration.

The shaped pulse power level was calibrated starting from 0.1 mW. The optimum value for the shaped pulse power level was 0.32 W.

To perform the UF-COSY experiment, the acquisition parameters set up for the encoding block were identical to those calibrated previously. The coherence selection gradients strength was 45 G/cm during 1000 ms, and the purge gradient strength was -10 G/cm with 400 ms duration. The acquisition times for direct and indirect dimensions were 65.59 and 0.12 ms, respectively. For the acquisition of 35 and -35.008 G/cm (to compensate for shearing effects), gradients were applied for 236 ms each, with a gradient rise time of 20 µs (recovery delay in pulse sequence).

For the UF-HSQC experiment, identical chirp pulses were used but applied in the presence of ± 20 G/cm encoding gradients to account for the larger ^{13}C frequency range. The acquisition times for direct and indirect dimensions were 65.59 and 0.02 ms, respectively. Acquisition gradients were identical to those employed for UF-COSY. The INEPT delay was set to 1.72 ms. Eight scans were recorded for sensitivity and phase-cycling purposes.

It is important to highlight that all hard pulses are calibrated in exactly the same way as for the conventional experiments.

Ultrafast spectra processing was performed by using an in-house routine in TopSpin®. This routine included conventional zero-filling and apodization features, including apodization in the ultrafast dimension (LB = -50 Hz and GM = 0.5) designed to optimize line shapes and sensitivity in the spatially-encoded dimension,[25] and also a Sine apodization function in the conventional dimension (LB = -8 Hz and GM = 0.08). Spectra were processed in magnitude mode.

The UF-COSY and UF-HSQC pulse sequence (Bruker format) are available in the supplementary material. The processing routine is freely available on demand.

Conventional 2D NMR parameters

The conventional COSY[33] and HSQC[34] 2D experiments were recorded using routine pulse sequence available in the Bruker TopSpin 3.1 software . The conventional COSY spectrum was performed in 6 scans, using 4096 data points (real + imaginary), 128 t_1 increments and a 2 s recovery delay. For the conventional HSQC, the number of t_1 increments was 128, with a recovery delay of 3 s, 4096 data points (real + imaginary) and a total of 8 scans.

RESULTS AND DISCUSSION

Calibration of encoding gradients and pulses

Spatially selective excitation is a fundamental step of UF-NMR experiments which needs to be carefully calibrated. Figure 1 describes the pulse sequence designed for this preliminary calibration. The first
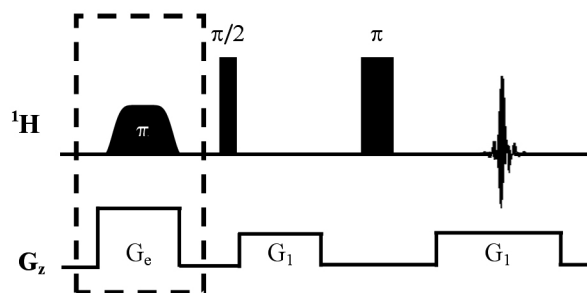

Figure 1. *Pulse sequence for calibration of the gradients needed for ultrafast 2D NMR experiments. The extra dashed block is appended to calibrate the chirp pulses needed for spatial encoding. Other experimental details, needed to implement this experiment, are included in the experimental section*

step consists of calibrating the excitation pulses in order to ensure that their frequency width matches the frequency dispersion induced by the excitation gradients (G_e).

A sample with only one resonance frequency (here H_2O in D_2O) should be used for more efficient calibration. First, the dashed block (pulse calibration stage) is inactivated by setting the G_e strength to 0.0 G/cm and the selective pulse power level to 0.0 W. The rest of the sequence generates a spin echo which, after Fourier transform, yields the excitation profile of the sample (Figure 2a). Because of the phase dispersion induced by the gradients, a large first-order phase correction followed by a small zero order correction, are necessary to obtain a symmetric image.
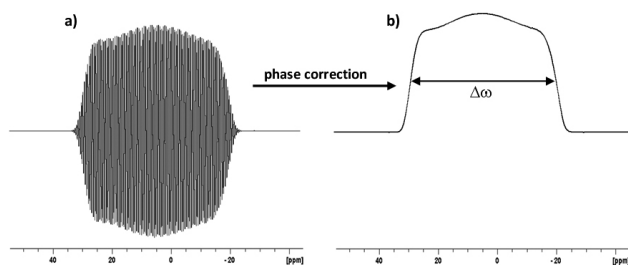

Figure 2. *Image of the excitation profile obtained from the pulse sequence in Figure 1 (without the extra block), allowing for gradient strength calibration. Without (a) and with (b) phase correction. The frequency dispersion Dω induced by G_2 is $\gamma \cdot G_2 \cdot L$, where γ is the gyromagnetic ratio of detected nuclei and L the height of the detection coil. For both spectra, the acquisition time, number of data points and number of scans were 12.58 ms, 2984 and 1, respectively. For the processing parameters, the window function was the Gaussian multiplication with line broadening of -20.0 and Gaussian maximum position of 0.5 for both spectra, while the phase corrections of zero and first order were set to zero for spectrum 2a and to $11x10^6$ and $-23x10^6$ for spectrum 2b*

The frequency dispersion induced by G_1 corresponds to the width of the excitation profile (Figure 2b). In order to perform ultrafast experiments, the gradient strength should be set to induce a frequency dispersion much higher than the chemical shift range, in order to ensure that all resonance frequencies are equally addressed at a given z position. Here, a 6.77 G/cm gradient is chosen, leading to a 54 kHz frequency dispersion, much higher than the usual ^1H spectral range. The next step consists of calibrating the adiabatic pulse used for spatial encoding. As discussed by Pelupessy,[20] its bandwidth should be slightly higher than the frequency dispersion induced by the gradients, to ensure that the whole sample is excited. The pulse calibration stage (Figure 1 - dashed block) is then activated, and the shaped pulse power level is decreased parametrically until complete inversion of the excitation profile is obtained (Figure 3S, supplementary material). In our case the optimum shaped pulse power level was 0.32 W. This gradient calibration procedure need be performed only once, so the optimized parameters can be used for other experiments.

UF-COSY 2D implementation

With both shaped pulse and encoding gradient properly calibrated, we proceed to the implementation of a homonuclear bidimensional NMR experiment: Ultrafast COSY (UF-COSY). The pulse sequence used is shown in Figure 4S, supplementary material. For the aforementioned reasons, the constant-time spatial encoding proposed by Pelupessy[20] was chosen to perform our experiments.

The UF-COSY pulse sequence starts with a nonselective π/2 pulse, followed by constant-time spatial encoding in which two adiabatic pulses are applied simultaneously with a bipolar excitation gradient pair (G_e), leading to a spatially selective encoding of the spins. As the

phase has a quadratic dependence on z^2 after the first chirp pulse,[20] it is necessary to apply a second pulse with an opposite gradient, to remove this effect and make the z-positions of the spins directly proportional to their resonance frequency. The mixing step is the same as for a conventional experiment, including coherence-selection gradients. A purge gradient (G_p) is used to shift the signal positions in the ultrafast dimension, in order to center them in the observation window. Finally, a bipolar acquisition gradient pair (G_a) is applied during $2.T_a$, to refocus the dephasing induced by the spatial encoding step, resulting in the formation of successive echoes according to the distinct precession frequency of the nuclei. This acquisition scheme is repeated N_2 times leading to complete sampling of the (k, t_2) space in a single scan. The acquisition gradient amplitude G_a should be chosen to ensure that the desired spectral width is observed in the spatially-encoded dimension. As a consequence, the maximum observable spectral width is limited by the maximum gradient amplitude available. While choosing $G_a = 100\%$ of the maximum gradient amplitude would ensure the observation of the largest spectral range possible, we recommend instead to first set $G_a = 70\%$ to avoid reaching the limits of the gradient hardware, principally to preserve its integrity but also because instabilities in the bipolar acquisition gradient train are observed for high G_a values. G_a can then be adjusted more finely depending on the spectral range to be detected.

Careful attention must be paid to shearing effects in the course of the acquisition process. Because of possible gradient offset, the positive acquisition gradient may not be the exact opposite of the negative gradient. This effect creates a linear shifting of the peak position during acquisition, leading to large resolution losses in the 2D spectrum. Therefore, fine tuning of the negative gradient amplitude must be performed to obtain optimum spectra.

An example of UF-COSY 2D spectrum is given in Figure 3b for a Levamisol sample. The spectrum is recorded in 0.17 s, whereas 30 min are necessary to record its conventional counterpart (Figure 3a). The two spectra exhibit the same homonuclear correlations, thus proving the efficiency of the ultrafast approach.
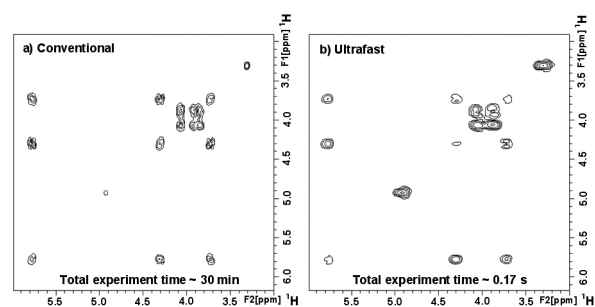

Figure 3. *(a) Conventional and (b) ultrafast COSY spectrum obtained on a 0.08 mol L^{-1} Levamisol sample in methanol, on a 400 MHz spectrometer at 298 K. The conventional spectrum was recorded with acquisition times of 365.96 ms (direct) and 11.43 ms (indirect), 4096 data points, 6 scans and 128 t_1 increments, and was processed using the sine-squared function with sine bell shift equals to 3 in both dimensions. The ultrafast spectrum was recorded in a single scan*

UF-HSQC 2D implementation

The pulse sequence for implementation of the heteronuclear 2D HSQC experiment (UF-HSQC) is described in Figure 5S, supplementary material. The spatial encoding stage was performed on the ^{13}C channel, therefore higher encoding gradients $\pm G_e$ were applied as described in the experimental part in order to account for the larger ^{13}C spectral range.

This UF-HSQC sequence has many steps in common with a conventional HSQC experiment. Initially, an INEPT block allows improving of the sensitivity of the ^{13}C nuclei by polarization transfer from the ^{1}H nuclei. Subsequently, spatial encoding is performed on the ^{13}C channel to permit the position-dependent evolution of the ^{13}C nuclei, and in the middle of this period, a π pulse is applied on the ^{1}H channel to refocus J_{CH} couplings. After a retro-INEPT block, the signal is detected on the ^{1}H channel. The echoes observed during the first acquisition gradient correspond to the ^{13}C spectrum, while the ^{1}H spectrum is obtained from the EPI dimension. Additionally, π pulses are added on the ^{13}C channel between acquisition gradients to perform ^{13}C decoupling.

As the ultrafast dimension window is limited by the strength of acquisition gradients, the spectral width observable in the ^{13}C dimension is limited to a few tens of ppm.[27] In order to overcome this limitation, the recently proposed "gradient-folding" method[27] to improve the spectral width of ultrafast 2D NMR experiments was used. The function of the gradients G_1 and G_2 is to enable the folding of the peaks that are outside the spectral window in the ultrafast dimension.

The spectrum obtained after performing this UF-HSQC pulse sequence on a 1-bromohexane sample is shown in Figure 4b. Eight transients were accumulated for the sake of sensitivity and to perform the conventional HSQC phase cycling for a more efficient coherence selection. However, the whole 2D spectrum is recorded in less than 1 minute, showing the same information as disclosed on the conventional spectrum (Figure 4a), but in a much shorter timeframe. The highlighted signal (13.9 ppm) in the ultrafast spectrum is folded in the ultrafast dimension by adjusting G_1 (30 G/cm) and G_2 (7.5 G/cm) gradients.
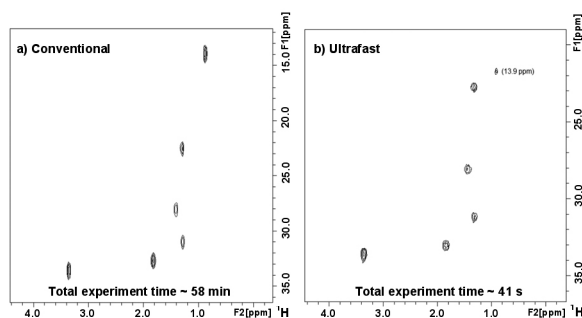

Figure 4. *(a) Conventional and (b) ultrafast HSQC spectrum obtained on a 2.37 mol L^{-1} 1-bromohexane sample in chloroform, on a 400 MHz spectrometer at 298 K. The conventional spectrum was recorded with acquisition times of 365.96 ms (direct) and 2.62 ms (indirect), 4096 data points, 8 scans and 128 t$_1$ increments, and was processed using the sine-squared function with sine bell shift equals to 2 in both dimensions. The ultrafast spectrum was recorded in 8 scans and there is a folded peak (13.9 ppm) indicated on this spectrum in order to overcome the aforementioned limitation of ultrafast spectral window*

CONCLUSIONS

This paper describes a detailed protocol for implementing both homo- and heteronuclear multidimensional ultrafast experiments. In spite of its impressive performance, it should be noted that ultrafast NMR is characterized by several limitations and compromises which potentially affect its performance. In particular, a trade-off has to be made between resolution, sensitivity and spectral width, as described in recent papers.[23,27,35] However, these limitations are now well understood, and solutions have been proposed to overcome them. These solutions include, for example, the use of multi-echo excitation to limit sensitivity losses due to molecular diffusion[24] or the use of k-space folding strategies to increase the accessible spectral width.[27,35]

The sensitivity issues of ultrafast 2D NMR are also an important point worth discussing. The sensitivity of a single-scan experiment is of course lower than that of a conventional experiment where signal is accumulated for minutes or hours. This single-scan sensitivity is clearly highly dependent on the spectrometer and probe, but typically 100 mM samples are used in 400 MHz instruments equipped with conventional probes, while 10 mM samples are commonly used in 500 MHz instruments equipped with cryogenic probes.[36] These values seem quite high, but lower concentrations are easily reached by signal averaging, a "multi-scan single shot" approach whose potentialities have been recently demonstrated.[37] Following these developments, ultrafast NMR has been recently applied to a variety of situations, such as monitoring of fast organic reactions,[28,38] the study of biologically relevant samples,[30,38] coupling with hyphenated techniques[39] and measurement of residual dipolar couplings in oriented media.[40]

We are currently applying these experiments to the study of dynamic processes occurring on a very short timescale that could not hitherto be followed by any other kind of 2D NMR experiment.

SUPPLEMENTARY MATERIAL

Free access in PDF format available on-line at http://quimicanova.sbq.org.br.

ACKNOWLEDGEMENTS

REFERENCES

1. Rabi, I.; Zacharias, J.; Millman, S.; Kusch, P.; *Phys. Rev.* **1938**, *53*, 318.
2. Bloch, F.; Hansen, W.; Packard, M.; *Phys. Rev.* **1946**, *69*, 127.
3. Purcell, E.; Torrey, H.; Pound, R.; *Phys. Rev.* **1946**, *69*, 37.
4. Jeener, J.; *International Ampere Summer School II,* Basko Polje, Yugoslavia, 1971.
5. Aue, W. P.; Karhan, J.; Ernst, R. R.; *J. Chem. Phys.* **1976**, *64*, 2229.
6. Lauterbur, P. C.; *Nature* **1973**, *242*, 190.
7. Mansfield, P.; Maudsley, A. A.; *J. Phys. C: Solid State Phys.* **1976**, *9*, L409.
8. Mandelshtam, V.; Taylor, H.; Shaka, A.; *J. Magn. Reson.* **1998**, *133*, 304.
9. Kupče, Ē.; Freeman, R.; *J. Magn. Reson.* **2003**, *162*, 300.
10. Brüschweiler, R.; Zhang, F.; *J. Chem. Phys.* **2004**, *120*, 5253.
11. Schanda, P.; Brutscher, B.; *J. Am. Chem. Soc.* **2005**, *127*, 8014.
12. Vitorge, B.; Bodenhausen, G.; Pelupessy, P.; *J. Magn. Reson.* **2010**, *207*, 149.
13. Frydman, L.; Scherf, T.; Lupulescu, A.; *Proc. Natl. Acad. Sci.* **2002**, *99*, 15858.
14. Gal, M.; Frydman, L. In *Encyclopedia of NMR*; Grant, D. M.; Harris, R. K., eds.; Wiley: New York, 2009, vol. 10.
15. Mishkovsky, M.; Frydman, L.; *Annu. Rev. Phys. Chem.* **2009**, *60*, 429.
16. Tal, A.; Frydman, L.; *Prog. Nuc. Magn. Res. Spec.* **2010**, *57*, 241.
17. Frydman, L.; Lupulescu, A.; Scherf, T.; *J. Am. Chem. Soc.* **2003**, *125*, 9204.
18. Shrot, Y.; Frydman, L.; *J. Magn. Reson.* **2003**, *164*, 351.
19. Shrot, Y.; Shapira, B.; Frydman, L.; *J. Magn. Reson.* **2004**, *171*, 163.
20. Pelupessy, P.; *J. Am. Chem. Soc.* **2003**, *125*, 12345.

21. Tal, A.; Shapira, B.; Frydman, L.; *J. Magn. Reson.* **2005**, *176*, 107.
22. Shrot, Y.; Frydman, L.; *J. Chem. Phys.* **2008**, *128*, 052209.
23. Giraudeau, P.; Akoka, S.; *J. Magn. Reson.* **2008**, *192*, 151.
24. Giraudeau, P.; Akoka, S.; *J. Magn. Reson.* **2008**, *190*, 339.
25. Pelupessy, P.; Duma, L.; Bodenhausen, G.; *J. Magn. Reson.* **2008**, *194*, 169.
26. Giraudeau, P.; Akoka, S.; *Magn. Reson. Chem.* **2011**, *49*, 307.
27. Giraudeau, P.; Akoka, S.; *J. Magn. Reson.* **2010**, *205*, 171.
28. Queiroz Jr, L. H. K.; Giraudeau, P.; dos Santos, F. A.; de Oliveira, K. T.; Ferreira, A. G.; *Magn. Reson. Chem.* **2012**, *50*, 496.
29. Giraudeau, P.; Lemeunier, P.; Coutand, M.; Doux, J.-M.; Gilbert, A.; Remaud, G. S.; Akoka, S.; *J. Spectrosc. Dyn.* **2011**, *1*, 2.
30. Lee, M.-K.; Gal, M.; Frydman, L.; Varani, G.; *Proc. Natl. Acad. Sci.* **2010**, *107*, 9192.
31. Frydman, L.; Blazina, D.; *Nat. Phys.* **2007**, *3*, 415.
32. Giraudeau, P.; Remaud, S.; Akoka, S.; *Anal. Chem.* **2009**, *81*, 479.
33. Nagayama, K.; Kumar, A.; Wüthrich, K.; Ernst, R. R.; *J. Magn. Reson.* **1980**, *40*, 321.
34. Bodenhausen, G.; Ruben, D. J.; *Chem. Phys. Lett.* **1980**, *69*, 185.
35. Shrot, Y.; Frydman, L.; *J. Chem. Phys.* **2009**, *131*, 224516.
36. Giraudeau, P.; Massou, S.; Robin, Y.; Cahoreau, E.; Portais, J-C.; Akoka, S.; *Anal. Chem.* **2011**, *83*, 3112.
37. Pathan, M.; Akoka, S.; Tea, I.; Charrier, B.; Giraudeau, P.; *Analyst* **2011**, *136*, 3157.
38. Pardo, Z. D.; Olsen, G. L.; Fernández-Valle, M. E.; Frydman, L.; Martínez-Álvarez, R.; Herrera, A.; *J. Am. Chem. Soc.* **2012**, *134*, 2706.
39. Queiroz Jr, L. H. K.; Queiroz, D. P. K.; Dhooghe, L.; Ferreira, A. G.; Giraudeau, P.; *Analyst* **2012**, *137*, 2357.
40. Giraudeau, P.; Montag, T.; Charrier, B.; Thiele, C. M.; *Magn. Reson. Chem.* **2012**, *50*, S53.

OPTIMIZATION AND PRACTICAL IMPLEMENTATION OF ULTRAFAST 2D NMR EXPERIMENTS

Luiz H. K. Queiroz Júnior*
Departamento de Química, Universidade Federal de São Carlos, Rod. Washington Luís, km 235, 13565-905 São Carlos – SP /
Instituto de Química, Universidade Federal de Goiás, CP 131, 74001-970 Goiânia – GO, Brasil
Antonio G. Ferreira
Departamento de Química, Universidade Federal de São Carlos, Rod. Washington Luís, km 235, 13565-905 São Carlos – SP, Brasil
Patrick Giraudeau
Université de Nantes, CNRS, Chimie et Interdisciplinarité: Synthèse, Analyse, Modélisation UMR 6230, B.P. 92208, 2 rue de la
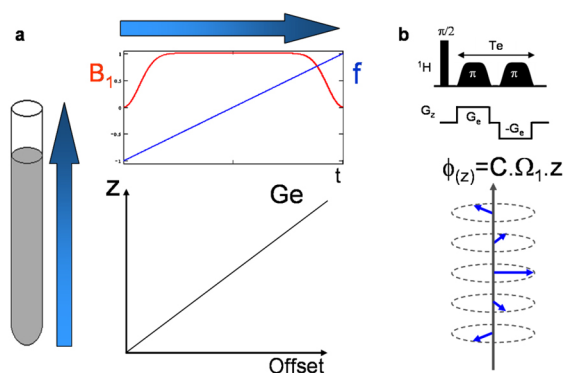Houssinière, F-44322 Nantes Cedex 03, France

Figure 1S. *(a) Graphical representation of continuous spatial encoding, in which a chirp pulse is applied concomitantly to a gradient pulse (G_e) along z axis. (b) The scheme proposed by Pelupessy[20] comprises the application of a 90º hard pulse followed by two π chirp pulses applied together with a bipolar pair of gradients*
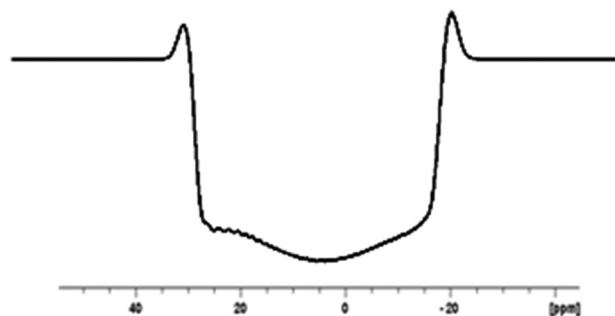

Figure 3S. *Image of the excitation profile obtained from the pulse sequence in Figure 1 (with the extra block) and after phase correction, allowing for the chirp pulse power calibration before performing ultrafast experiments. The acquisition and processing parameters are the same mentioned for the Figure 2b, unless the chirp pulse power that was 0.32 W*
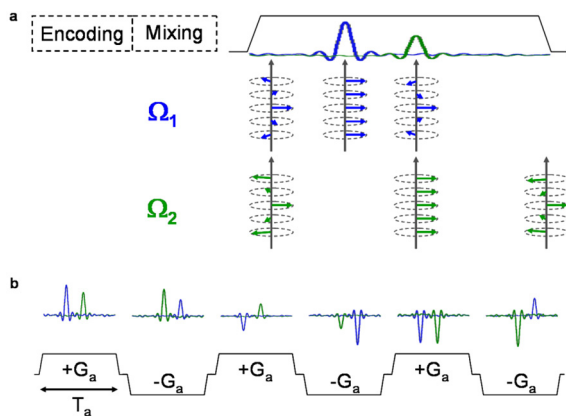

Figure 2S. *(a) Representation of the ultrafast dimension acquisition by the application of a gradient pulse, in order to remove the dephasing created during the spatial encoding step. As result, the echo peaks are formed as the dephasing is being refocused. (b) Representation of the conventional dimension acquisition by the use of a bipolar pair of gradient pulses, which results in the monitoring of conventional parameters evolution as a series of sub-spectra are being collected*
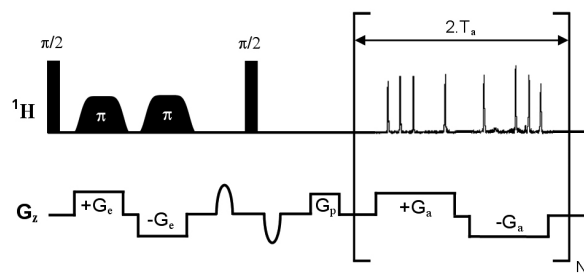

Figure 4S. *Ultrafast COSY pulse sequence based on the constant-time spatial encoding scheme proposed by Pelupessy.[20] To perform this experiment, the coherence selection gradients strength was 45 G/cm during 1000 µs, and the purge gradient strength was -10 G/cm with 400 µs of duration. The acquisition times for direct and indirect dimensions were 65.59 and 0.12 ms, respectively. For the acquisition 35 and -35.008 G/cm (to compensate for shearing effects) gradients were applied for 236 µs each, with a gradient rise time of 20 µs (recovery delay in pulse sequence)*
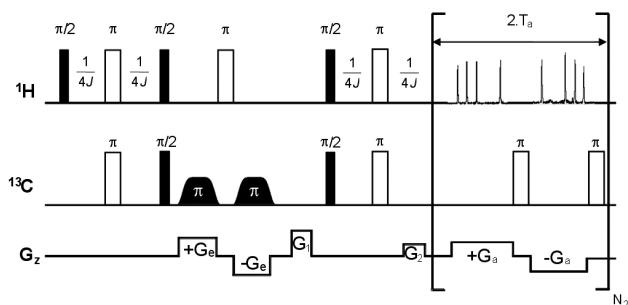
*e-mail: professorkeng@gmail.com

Figure 5S. *Ultrafast HSQC pulse sequence based on the constant-time spatial encoding scheme proposed by Pelupessy.[20] An asymmetric phase cycle (x,-x,x,x) was used within each single shot acquisition on the decoupling pulse to avoid the formation of decoupling artifacts. It was also used a real phase cycle (x,-x), requiring several scans, on the last ^{13}C 90º pulse and the receiver. To perform this experiment, identical chirp pulses than those for UF-COSY were used, but applied in the presence of ± 20 G/cm encoding gradients to account for the larger ^{13}C frequency range. The acquisition times for direct and indirect dimensions were 65.59 and 0.02 ms, respectively. Acquisition gradients were identical to those employed for UF-COSY. The INEPT delay was set to 1.72 ms. Eight scans were recorded for sensitivity and phase-cycling purposes*

PULSE SEQUENCE FOR UF-COSY

```
;ufcosy
;avance-version

;$CLASS=HighRes
;$DIM=1D
;$TYPE=
;$SUBTYPE=
;$COMMENT=

#include <Avance.incl>
#include <Grad.incl>
#include <De.incl>

1 ze
  100u UNBLKGRAD
2 d1 pl1:f1
  p1 ph1                      → 90º pulse
  10u gron0              ⎫
  p11:sp1:f1 ph2         ⎪
  10u groff              ⎪
  10u gron1              ⎬   spatial encoding block
  p11:sp1:f1 ph4         ⎪
  10u groff              ⎭
  10u pl1:f1
  10u
  p23:gp23                    → coherence selection gradient
  10u
  p1 ph1                      → mixing period
  10u
  p26:gp26                    → coherence selection gradient
  d25 gron25                  → purge gradient
  10u groff
  10u
  ACQ_START(ph30,ph31)   ⎫   starting acquisition
  1u DWELL_GEN:f1        ⎭
3 d20 gron2                   → positive acquisition gradient
```

```
  d6 groff          ⟶   gradient recovery delay
  d20 gron3         ⟶   negative acquisition gradient
  d6 groff          ⟶   gradient recovery delay
  lo to 3 times l3  ⟶   loop for acquisition
  rcyc=2
  100u BLKGRAD
  30m mc #0 to 2 F1QF(ip10, id0)
exit


ph1=0
ph2=0
ph4=2
ph30=0
ph31=0
```

PULSE SEQUENCE FOR UF-HSQC

```
;ufhsqc
;avance-version

;$CLASS=HighRes
;$DIM=2D
;$TYPE=
;$SUBTYPE=
;$COMMENT=

#include <Avance.incl>
#include <Grad.incl>
#include <De.incl>

"p2=p1*2"
"p4=p3*2"
"d4=1s/(cnst2*4)"
"d6=d4-d15"
"d10=p20"
"d11=p21"
"p15=(td*dw)/(2*l3)-2*d17-p4"
1 ze
  100u UNBLKGRAD
2  30m pl2:f2
  d1 pl1:f1
  p1 ph0                 ⎫
  d4                     ⎪
  (center (p2 ph1) (p4 ph4):f2 )  ⎬   INEPT block
  d4                     ⎪
  p1 ph2                 ⎪
  (p3 ph3):f2            ⎭
  d11
  10u gron0              ⎫
  p7:sp1:f2 ph1          ⎪
  10u groff              ⎪
  d10                    ⎪
  10u                    ⎬   spatial encoding block
  p2 ph1                 ⎪   → 180º pulse
  10u                    ⎪
  10u gron1              ⎪
  p7:sp1:f2 ph1          ⎪
  10u groff              ⎭
  d14 gron4 pl2:f2   ⟶   coherence selection and folding gradient
  10u groff
```

```
(p3 ph5):f2   ⎫
(p1 ph1)      ⎬  retro-INEPT block
d4            ⎪
(center (p2 ph1) (p4 ph4):f2 ) ⎭
d6
d15 gron5     ⟶  coherence selection and folding gradient
10u groff
10u
d15 gron7     ⟶  purge gradient
10u groff
ACQ_START(ph30,ph31) ⎫
1u DWELL_GEN:f1      ⎬ starting acquisition
3 p15:gp15    ⟶  positive acquisition gradient
d17           ⟶  recovery delay
(p4 ph6):f2   ⟶  decoupling pulse
d17           ⟶  recovery delay
p15:gp16      ⟶  negative acquisition gradient
d17           ⟶  recovery delay
(p4 ph6):f2   ⟶  decoupling pulse
d17 ipp6      ⟶  recovery delay / phase (ph6) increment
```

```
lo to 3 times l3  ⟶  loop for acquisition
rcyc=2
100u BLKGRAD
30m mc #0 to 2 F1QF(id2)
exit

ph0=0
ph1=0
ph2=1
ph3=0
ph4=0
ph5=0 2
ph6=0 2 0 0  ⟶  asymmetric phase cycle on the
                decoupling pulse to avoid the formation
                of decoupling artifacts
ph7=1
ph8=3
ph30=0
ph31=0 2
```